J Sol-Gel Sci Technol (2016) 78:365–372
DOI 10.1007/s10971-016-3966-7

ORIGINAL PAPER: SOL-GEL AND HYBRID MATERIALS FOR CATALYTIC, PHOTOELECTROCHEMICAL AND SENSOR APPLICATIONS

Structural, morphological and optical properties of tin oxide nanoparticles synthesized by sol–gel method adding hydrochloric acid

Subramaniam Mohana Priya[1] · A. Geetha[1] · K. Ramamurthi[1]

Received: 19 September 2015 / Accepted: 18 January 2016 / Published online: 5 February 2016

Abstract Tin oxide (SnO_2) nanoparticles were synthesized by sol–gel method from cost-effective tin chloride ($SnCl_2{\cdot}2H_2O$) and ethanol by adding ammonia solution. In a separate experiment, 4 ml of concentrated hydrochloric acid was added to this solution and SnO_2 nanoparticles were prepared. Further SnO_2 nanoparticles prepared without and with adding the hydrochloric acid were annealed at 200 °C for 1 h. The structural, morphological and optical properties of the synthesized SnO_2 nanoparticles were studied by X-ray diffraction, scanning electron microscope, UV–Vis spectroscopy, Fourier transform infrared spectroscopy and fluorescence spectroscopy techniques. As prepared SnO_2 nanoparticles by adding hydrochloric acid in the synthesis process reduced the crystallite size to ~4 from ~10 nm size of the annealed SnO_2 nanoparticles prepared without adding hydrochloric acid. Annealing the SnO_2 nanoparticles prepared adding hydrochloric acid improved the crystallite size from ~4 to ~4.5 nm. Addition of hydrochloric acid effectively modified the morphology of the SnO_2 nanoparticles from agglomerated spherical structure to cauliflower-like structure. The band gap is increased due to decrease in the crystallite size in the sample prepared adding hydrochloric acid. Fluorescence spectrum exhibits a strong emission peak at 350 nm. Addition of HCl plays a major role to suppress the hydrolysis rate and leads to the formation of SnO_2 nanoparticles.

✉ A. Geetha
geetha.phys@gmail.com

[1] Crystal Growth and Thin Film Laboratory, Department of Physics and Nanotechnology, Faculty of Engineering and Technology, SRM University, Kattankulathur, Tamil Nadu 603203, India

Graphical Abstract

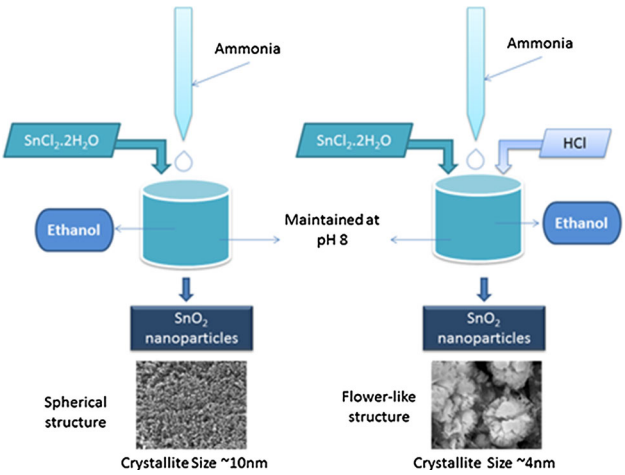

Keywords Semiconductors · SnO_2 nanoflowers · Hydrochloric acid · Ethanol · Optical properties · FL emission

1 Introduction

Improved properties of semiconductor metal oxides make them to find applications in many fields. Among the semiconducting metal oxides tin oxide (SnO_2) has been widely investigated because of its wide band gap of 3.6 eV and its potential applications in various fields like gas sensors, solar cells, liquid crystal displays and photovoltaic cells [1–4]. The physical and chemical properties of the synthesized materials are also influenced by their crystalline or amorphous nature [3]. The size-dependent properties of SnO_2

nanoparticles in tuning the electrical, morphological and optical properties are very important [5]. In addition to low dimensional SnO_2 nanostructures, literature show reports on the nanorods [6], nanobelts [7] and nanowires [8] prepared by using various synthesis methods. Many synthesis methods are employed to tailor the properties of nanostructured SnO_2 which paved the way for several applications [9]. Jitianu et al. [10] prepared SnO_2 nanoparticles by sol–gel method using di-*n*-butyl-tin-bis-acetylacetonate with the addition of HCl and reported larger crystallite size ($\sim$21–28 nm). Talebian et al. [11] employed solvothermal method and reported synthesis of SnO_2 nanoparticles with different morphology using various surfactants. Kaneti et al. [12] reported the formation of flower-like SnO_2 nanorods by solvothermal method for high reaction time. Pal and Chauhan [13] reported the preparation of SnO_2 nanoparticles employing surfactant mediated method using cetyltrimethyl ammonium bromide (CTAB) as a surfactant where $SnCl_4{\cdot}2H_2O$ as a precursor and obtained reduced crystallite size (7–8 nm) with increased band gap. Lupan et al. [14] reported one-dimensional SnO_2 nanorods synthesized by hydrothermal method with high yield and controlled morphology. Azham et al. [15] reported that on increasing Mn concentration the crystallite size of SnO_2 nanoparticles is reduced, whereas the band gap is increased. Nehru et al. [16] synthesized, SnO_2 nanoparticles by chemical precipitation method and obtained spherical-shaped structure and reported that annealing temperature increased the crystallite size. Anandan and Rajendiran [17] reported the synthesis of HCl added SnO_2 nanoparticles by solvothermal method on varying the reaction temperature which leads to decrease in crystallite size and increase in band gap. In the present work, we report for the first time the synthesis of SnO_2 nanoparticles of $\sim$4 nm size from the tin chloride ($SnCl_2{\cdot}2H_2O$) employing the cost-effective sol–gel method without adding any surfactant but adding $\sim$4 ml of hydrochloric acid in the synthesis process.

2 Materials and methods

All chemicals were purchased from Emerck with analytical reagent grade (99.99 % purity). Most of the previous works report the synthesis of tin oxide nanoparticles from tin tetrachloride pentahydrate ($SnCl_4{\cdot}5H_2O$) [18–20], but in this work SnO_2 nanoparticles were synthesized from the cost-effective tin dichloride dihydrate ($SnCl_2{\cdot}2H_2O$). Further in the present work we report on the preparation of SnO_2 nanoparticles with and without adding hydrochloric acid. The effect of hydrochloric acid addition in the synthesis process of SnO_2 nanoparticles can be explained as follows: the effect of HCl addition on the oxidation states of tin oxide is associated with the hydrolysis of $SnCl_2$ in the solvent [21]. Donaldson et al. [22] reported that the $Sn_4(OH)_2Cl_6$ colloidal particles are formed as a result of hydrolysis of $SnCl_2$ reaction, if the pH of the $SnCl_2$ solution is between 1.24 and 4.13. Addition of sufficient amount of HCl in the tin chloride solution makes the $SnCl_2$ solution transparent. This indicates that in the $SnCl_2$ solution, no Sn_4 $(OH)_2$ Cl_6 colloidal particles exists but tin composition exists as Sn^{2+} cations which leads to the formation of SnO_2 phase. The formation of SnO_2 phase is due to the reaction between Sn^{2+} cations and dissolved oxygen in the solution [23]. If the amount of HCl is increased then the rate of hydrolysis seems to be fast and aggregation of small SnO_2 nanoparticles is produced. Thus the addition of HCl reduces the SnO_2 particle size and introduces the quantum confinement effect due to more surfaces to volume ratio.

Initially, 1.1 g of $SnCl_2{\cdot}2H_2O$ was taken and dissolved in 50 ml of ethanol. Then it was stirred and on stirring ammonia solution was added drop by drop to maintain a pH 8. The product was centrifuged and dried in hot air oven at 60 °C for 4 h. Then the product was annealed at 200 °C for 1 h which yielded SnO_2 nanoparticles (named as SnO_2 ANLD). $SnCl_2{\cdot}2H_2O$ 1.1 g was taken in a beaker and about 4 ml of concentrated hydrochloric acid was added to this and was heated and kept at about 60 °C for 5 min. Then it was allowed to cool to the room temperature. 50 ml of ethanol was added to it, and the solution was stirred. On stirring this solution ammonia solution was added drop wise to obtain and maintain a pH 8. Then the product was centrifuged and dried in hot air oven at 60 °C for 4 h which yielded SnO_2 nanoparticles [named as SnO_2 (HCl)]. Then SnO_2 (HCl) was annealed at 200 °C for 1 h [named as SnO_2 (HCl ANLD)]. Then SnO_2 (ANLD), SnO_2 (HCl) and SnO_2 (HCl ANLD) nanopowders were characterized for the structural and optical properties. X-ray diffraction (XRD) pattern of the samples was recorded using X-ray diffractometer (X'Pert PAN Analytical) with CuK_α radiation ($\lambda = 1.5405$ Å). Morphology of the synthesized tin oxide nanoparticles was studied using FEI Quanta FEG 200 scanning electron microscope (SEM). Optical properties were studied using UV–Vis spectrophotometer (Shimadzu 2450), and Fourier transform infrared (FT-IR) spectrum was recorded using ALPHA-T FT-IR Spectrometer. Fluorescence spectrum was recorded using Jasco FP-6300 Spectrofluorometer with 150 W Xenon lamp.

3 Results and discussion

3.1 Structural studies

Figure 1 shows the XRD pattern of (a) SnO_2 (ANLD), (b) SnO_2 (HCl) and (c) SnO_2 (HCl ANLD) nanoparticles. XRD peaks are compared with JCPDS file (no: 41-1445)

and are indexed (Fig. 1) which reveal that the SnO_2 nanoparticles belong to the tetragonal system. Addition of a 4 ml of HCl in the synthesis process produced weak and broad XRD peaks which show that addition of a 4 ml HCl is effectively reduced the crystallite size of SnO_2. Further annealing the SnO_2 (HCl) nanoparticles at 200 °C for 1 h slightly improves the crystallinity. Previous report shows that the crystallinity of the synthesized SnO_2 nanoparticles is increased on annealing at 300 °C [24]. When compared with the XRD peaks of SnO_2 (ANLD) the intensity of the peaks decreased and they become broader in SnO_2 (HCl) sample. The XRD pattern clearly shows that (200) and (220) peaks observed in SnO_2 (ANLD) disappeared in SnO_2 (HCl) nanoparticles due to addition of HCl in the process of synthesis. The lattice parameters were calculated using $1/d^2 = (4\sin^2\ \theta)/\lambda^2 = (h^2 + k^2)/a^2 + l^2/c^2$ where a and c are the unit cell parameters and d is the interplanar distance [25]. The calculated values $a = 4.73$ Å (4.73 Å) and $c = 3.16$ Å (3.18 Å) compare well with the reported values by Tan et al. [3] given in the parenthesis. The average crystallite size was calculated from XRD pattern using Debye–Scherrer formula, $D = 0.9\ \lambda/(\beta \cos \theta)$, where λ is the wavelength of X-rays used (1.5405 Å), β is the Full Width Half Maximum (FWHM) in radian and θ is the angle of diffraction [25]. The average crystallite size calculated from (110), (101) and (211) peaks of SnO_2 (ANLD), SnO_2 (HCl) and SnO_2 (HCl ANLD) nanoparticles is, respectively, about 10.3, 4.1 and 4.5 nm. Previous report on the synthesis of tin oxide nanoparticles using the CTAB as the surfactant shows that the crystallites of ~7–8 nm size were obtained [13]. The crystallite size of SnO_2 nanoparticles obtained in this work is compared with that of the previous works in Table 1. Thus, the values given in Table 1 evidently show that addition of a 4 ml of HCl in the synthesis process effectively reduced the size of the SnO_2 crystallites to 4.1 nm and the process of annealing these particles at 200 °C yielded crystallite size of ~4.5 nm. Further the crystallite size obtained in this work seems to be the smallest when compared with the previous reports which used different surfactants (Table 1).

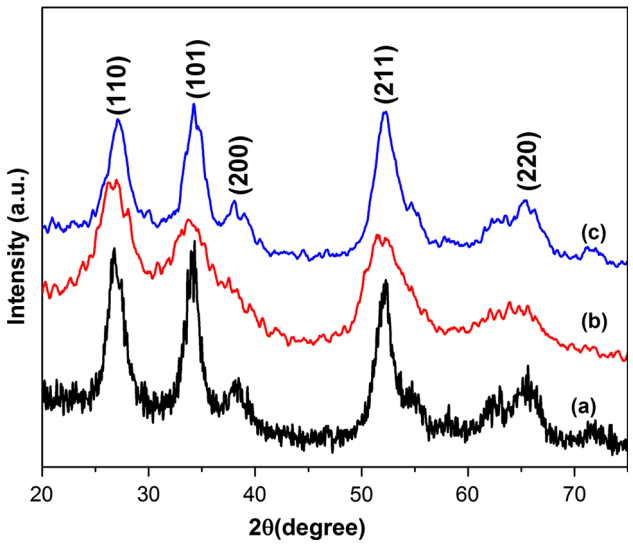

Fig. 1 XRD pattern of *a* SnO_2 (ANLD), *b* SnO_2 (HCl), *c* SnO_2 (HCl ANLD) nanoparticles

3.2 Morphological analysis

Figure 2 shows the SEM images of the surface morphology of (a) SnO_2 (ANLD), (b) SnO_2 (HCl) and (c) SnO_2 (HCl ANLD) nanoparticles. SEM image of SnO_2 (ANLD) shows that the spherical particles are agglomerated and spread densely on the surface with observable pinholes. The SnO_2 nanoparticles synthesized by adding a 4 ml of HCl [SnO_2 (HCl)] exhibit cauliflower-like structures. Earlier work also shows that addition of different surfactants like CTAB and sodium dodecyl sulfate (SDS) gives flower-like structures [26]. The average particle size of SnO_2 (HCl) nanoparticles calculated from SEM results is ~2.34 μm. The SnO_2 (HCl) nanopowders annealed at 200 °C for 1 h show uniformly distributed nearly spherical-shaped agglomerations of nanoparticles on the film surface with holes. Thus the cauliflower-like structures obtained for SnO_2 (HCl) are modified into agglomerated nearly spherical-shaped nanoparticles. One can observe that SnO_2 (ANLD) and SnO_2 (HCl ANLD) SEM images show similarity on their surface structure. Figure 3 shows the energy-dispersive X-ray analysis (EDX) of the SnO_2 (ANLD), SnO_2 (HCl) and SnO_2 (HCl ANLD) tin oxide nanoparticles. The EDAX spectrum shows clearly the presence of tin and oxygen elemental peaks.

3.3 Optical properties

The UV–Vis absorbance spectra of the (a) SnO_2 (ANLD), (b) SnO_2 (HCl) and (c) SnO_2 (HCl ANLD) nanoparticles are given in Fig. 4. Generally, the semiconductor nanoparticles undergo quantum confinement which depends on the size of the particles. The band gap of materials is increased, when the particle size is decreased and the absorption edge is shifted toward the higher energy side [13, 28]. When the size of SnO_2 nanoparticles is smaller than the exciton Bohr radius, there will be the occurrence of quantum confinement and the blue shift [29]. Accordingly, in the present work, the absorption peak observed at 294 nm for the SnO_2 (ANLD) nanoparticles is shifted to 276 nm for SnO_2 (HCl) nanoparticles, thus indicating a blue shift due to the effect of quantum confinement. When the SnO_2 (HCl) nanoparticles were annealed the absorption edge is shifted to 361 nm, thus

Table 1 Comparison of crystallite size, morphology, band gap and FL emission of SnO_2 nanoparticles

SnO_2 nanoparticles	Crystallite size (nm)	Morphology	Band gap (E_g) eV	FL emission (nm)	References
SnO_2(ANLD)	10.3	Spherical	3.6	433	PW
SnO_2 (HCl)	4.1	Cauliflower	4.3		
SnO_2 (HCl ANLD)	4.5	Spherical	3.7		
(SnO_2)-					
SDS	8	Flower petal	3.9	395	[26]
CTAB	11	Cauliflower	3.93		
PEG	13	Sheets and rods	3.8		
(SnO_2)-					
SDS	5	Spherical	3.83	390	[27]
CTAB	6.2		3.80		
PEG	10		3.78		
(SnO_2)-					
CTAB	81	Cauliflower	2.2	–	[11]
SDS	85	Flower petal	2.41		
(SnO_2)-					
CTAB	7–8	–	4.0	526	[13]
				565	
(SnO_2)	8–43	Spherical	–	417	[16]

PW Present work, *CTAB* cetyltrimethyl ammonium bromide, *SDS* sodium dodecyl sulfate, *PEG* polyethylene glycol

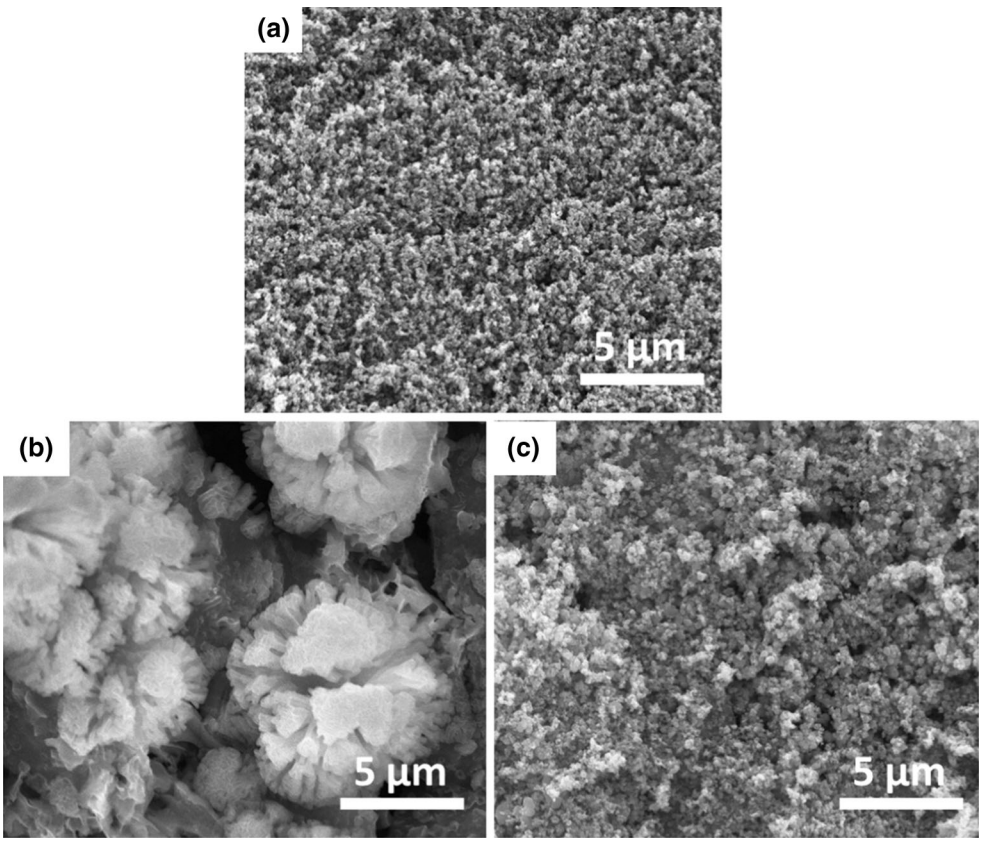

Fig. 2 SEM images of **a** SnO_2 (ANLD), **b** SnO_2 (HCl) and **c** SnO_2 (HCl ANLD) nanoparticles

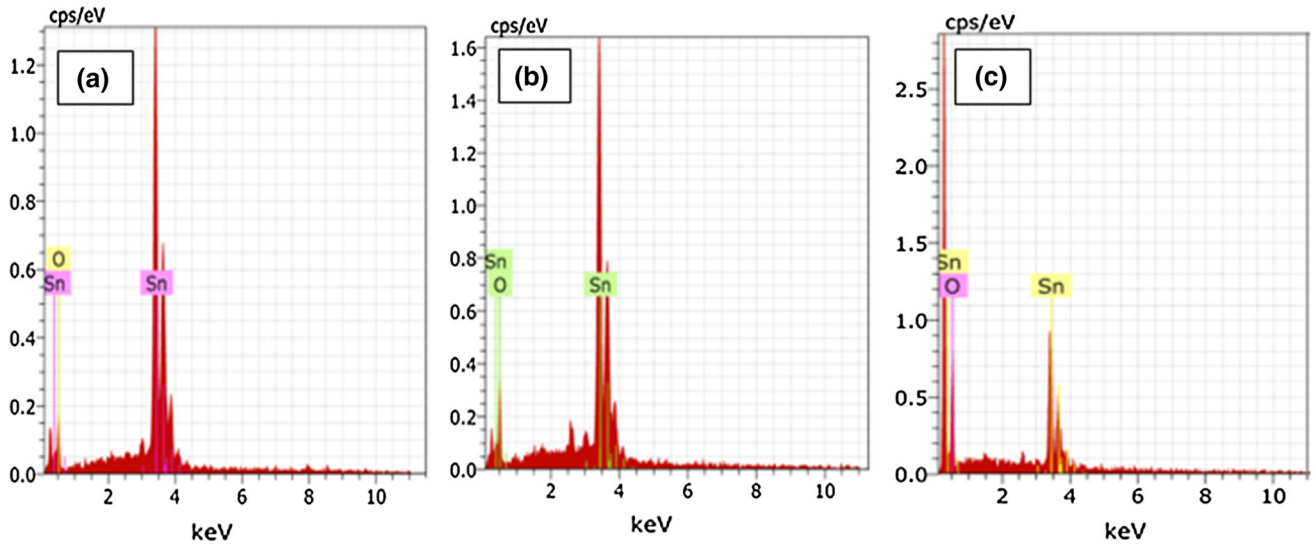

Fig. 3 Elemental analysis of **a** SnO_2 (ANLD), **b** SnO_2 (HCl) and **c** SnO_2 (ANLD) nanoparticles

indicating a red shift in the SnO_2 (HCl ANLD) when compared to that of SnO_2 (ANLD). The band gap is calculated using the formula, $\alpha h\nu = B(h\nu - E_g)^n$, where n takes the value of ½ for direct transition, B is a constant called band tailing parameter, and $h\nu$ is the incident photon energy [30]. The direct band gap was estimated using Tauc plot which is plotted between $h\nu$ and the $(\alpha h\nu)^2$. Figure 5 shows the band gap of SnO_2 (ANLD), SnO_2 (HCl) and SnO_2 (HCl ANLD) nanoparticles. The direct band gap of (a) SnO_2 (ANLD), (b) SnO_2 (HCl) and (c) SnO_2 (HCl ANLD) nanoparticles is 3.6, 4.3 and 3.7 eV, respectively. It is evident from the literature that increase in band gap is associated with decrease in particle size [29]. The direct band gap value obtained in this work is compared with the values of the earlier reports in Table 1. The results evidently show that relatively small size SnO_2 nanoparticles of about ~4.1 nm obtained by adding HCl in the synthesis process gives relatively higher band gap of 4.3 eV.

3.4 FTIR analysis

Figure 6 presents the room temperature FTIR spectrum recorded using KBr pellet technique in the wavelength range 4000–500 cm^{-1} for (a) SnO_2 (ANLD) (b) SnO_2 (HCl) and (c) SnO_2 (HCl ANLD) nanoparticles. The absorption band observed at ~3400 cm^{-1} [SnO_2 (HCl ANLD)], 3413 cm^{-1} [SnO_2 (HCl)] and 3396 cm^{-1} [SnO_2 (ANLD)] is due to

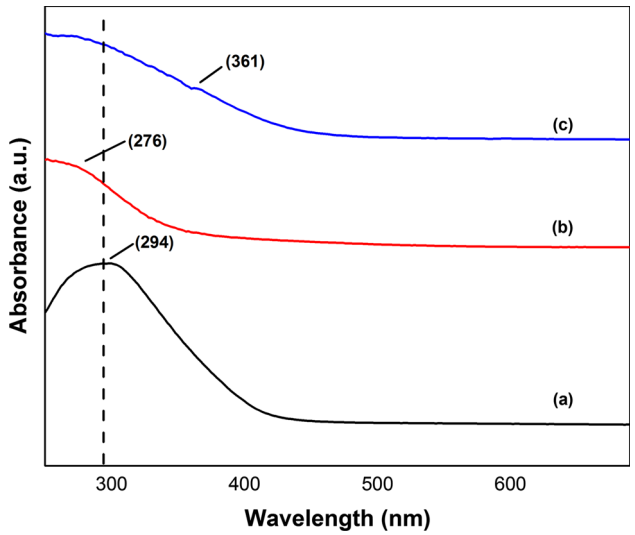

Fig. 4 UV–Vis absorbance spectra for *a* SnO_2 (ANLD), *b* SnO_2 (HCl) and *c* SnO_2 (HCl ANLD) nanoparticles

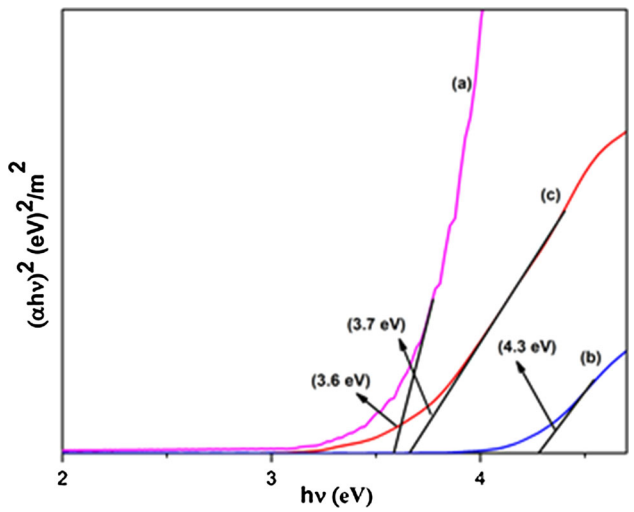

Fig. 5 Band gap of *a* SnO_2 (ANLD), *b* SnO_2 (HCl), and *c* SnO_2 (HCl ANLD) nanoparticles

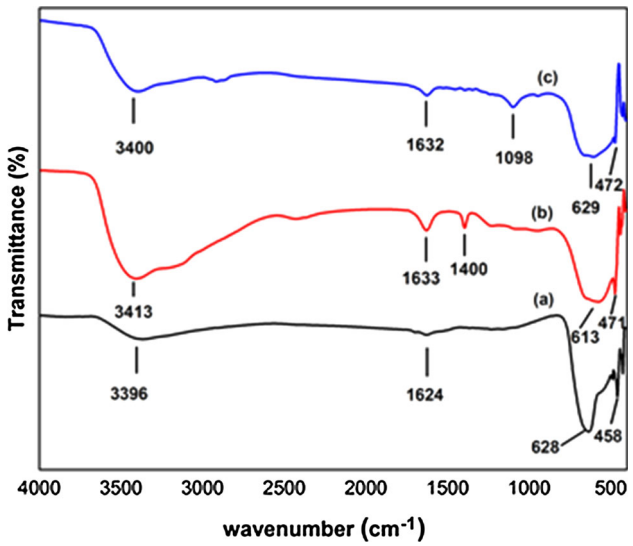

Fig. 6 FT-IR spectrum of *a* SnO_2 (ANLD), *b* SnO_2 (HCl), and *c* SnO_2 (HCl ANLD) nanoparticles

O–H antisymmetric stretching vibration of water molecules [31, 32]. The band observed at ~1624 cm^{-1} [SnO_2 (ANLD)], 1633 cm^{-1} [SnO_2 (HCl) and 1632 cm^{-1} [SnO_2 (HCl ANLD)] is due to the bending vibration of water molecules [18, 32]. The peak observed at 1400 cm^{-1} in SnO_2 (HCl) is correlated with NH_3, and when it is annealed at 200 °C makes the band at 1400 cm^{-1} to more weaker in [SnO2 (ANLD)], and [SnO2 (HCl ANLD)] [18]. In the sample SnO_2 (HCl ANLD), a new peak is present at ~1098 cm^{-1} which is due to the vibrations of O–O bond in the ion radical stabilized on Sn^{2+} [33]. A broad peak at ~613 cm^{-1} is due to the antisymmetric Sn–O–Sn stretching mode of the surface-bridging oxide formed by hydroxyl groups [34]. The FT-IR spectra of the samples give vibrational frequencies at 628 and 458 cm^{-1} (SnO_2 ANLD), 613 and 471 cm^{-1} (SnO_2 HCl) and 629 and 472 cm^{-1} [SnO_2 (HCl ANLD)] which represent the characteristic metal oxygen vibrational frequency [35]. The peak appeared at 628, 613 and 629 cm^{-1} in all the three samples are due to O–Sn–O bridge functional group which clearly indicates the formation of SnO_2 phase [3, 36].

3.5 Fluorescence studies

Room temperature fluorescence (FL) spectra of the SnO_2 (ANLD), SnO_2 (HCl) and SnO_2 (HCl ANLD) nanoparticles recorded in the range of 400–500 nm are given in Fig. 7. The excitation of SnO_2 nanoparticles is observed at ~331 nm for all the synthesized samples (Fig. 7A). The excitation wavelength of 331 nm produced a strong emission peak at ~350 nm and a weak emission peak at ~432 nm in all three samples is attributed to defects levels in the band gap such as oxygen vacancies [18]. In the case of [SnO_2 (HCl)], the emission peak is observed at ~345 nm and weak peak is observed at ~432 nm. In the sample [SnO_2 (HCl ANLD)], a weak emission peak is appeared at ~433 nm in addition to the peak at ~350 nm. Thus, the FL spectra evidently show that there is no appreciable changes in the position of the peak for all the samples but the intensity of SnO_2 (HCl) is relatively high due to less crystallite size among the three SnO_2 samples. On the whole, the emission peak at ~345 nm is observed with maximum intensity for the SnO_2 (HCl) sample, which is assigned to near band-edge emission [37]. The peaks become broader for both the SnO_2 (HCl) and SnO_2 (HCl ANLD) than that of the SnO_2 (ANLD) nanoparticles because of the influence of HCl on the crystallite size as observed from the results of XRD.

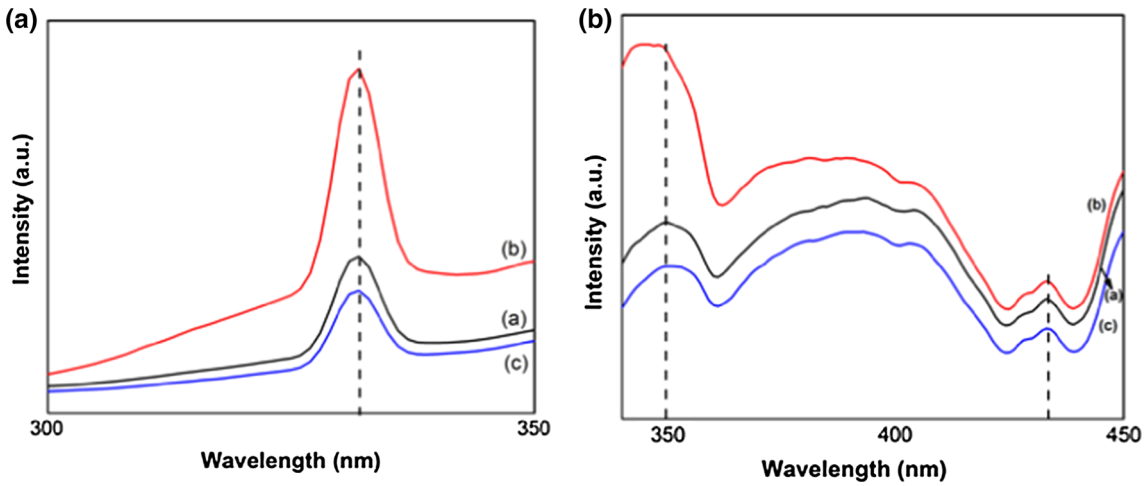

Fig. 7 Fluorescence of **A** excitation and **B** emission spectra of (*a*) SnO_2 (ANLD), (*b*) SnO_2 (HCl), and (*c*) SnO_2 (HCl ANLD) nanoparticles

4 Conclusions

Crystallite size of SnO_2 nanoparticles of $\sim$10 nm is prepared by sol–gel method is decreased effectively to $\sim$4.1 nm due to the addition of HCl in the process of synthesis. Further, annealing the SnO_2 (HCl) sample at 200 °C for 1 h is improved the crystallinity from $\sim$4.1 to 4.5 nm as has been observed from XRD results. SEM images show a marked difference in morphology of the samples prepared with and without HCl. Addition of HCl in the synthesis process of SnO_2 nanoparticles modified the surface morphology into flower-like structure and increased the band gap to 4.3 eV. Annealing the SnO_2 (HCl) samples at 200 °C gives uniformly distributed spherical-shaped SnO_2 nanoparticles on its surface and reduces the band gap from 4.3 to 3.7 eV. The UV–Vis spectral analysis shows that addition of HCl in the synthesis process enhances the intensity of FL peak at $\sim$350 nm, due to decrease in particle size and hence an increase in the band gap of the synthesized nanoparticles which could be useful for the optoelectronic and gas sensing applications. The results of the present work show that addition of HCl in the synthesis process effectively reduces the crystallite size of the as synthesized SnO_2 nanoparticles which is relatively smaller when compared with that the previous works, assisted by various capping agents in the synthesis process.

Acknowledgments One of the authors (M P) sincerely thanks SRM University, Chennai, for the award of SRM research fellowship to carry out the work. The authors gratefully acknowledge Prof. D. John Thiruvadigal, Head Department of Physics and Nanotechnology, SRM University, for extending the facilities created under (DST-FIST SR/FST/PSI-155/2010). The authors also thank Centre for Nanoscience and Nanotechnology and also to Nanotechnology Research Centre, SRM University, for extending the characterization facilities and to Prof. S. Moorthi Babu Crystal Growth Centre, Anna University, for extending the experimental facility to record FL spectra. The authors also thank Dr. A. Karthigeyan Asst. Prof., SRM University, for his kind support and valuable suggestions.

References

1. Reddy AS, Figueiredo NM, Cavaleiro A (2013) Nanocrystalline Au:Ag:SnO_2 films prepared by pulsed magnetron sputtering. J Phys Chem Solids 74:825–829
2. Pires FI, Joanni E, Savu R, Zaghete MA, Longo E, Varela JA (2008) Microwave-assisted hydrothermal synthesis of nanocrystalline SnO powders. Mater Lett 62:239–242
3. Tan L, Wang L, Wang Y (2011) Hydrothermal synthesis of SnO_2 nanostructures with different morphologies and their optical properties. J Nano Mater 10 pp
4. Wang CT, Chen HY, Chen YC (2013) Gold/vanadium–tin oxide nanocomposites prepared by co-precipitation method for carbon monoxide gas sensors. Sens Actuators B Chem 176:945–951
5. Feng YS, Zhou SM, Li Y, Li CC, Zhang LD (2003) Synthesis and characterization of tin oxide nanoparticles dispersed in monolithic mesoporous silica. Solid State Sci 5:729–733
6. Chen D, Gao L (2004) Facile synthesis of single-crystal tin oxide nanorods with tunable dimensions via hydrothermal process. Chem Phys Lett 398:201–206
7. Cheng Y, Yang R, Zheng JP, Wang ZL, Xiong P (2012) Characterizing individual SnO_2 nanobelt field-effect transistors and their intrinsic responses to hydrogen and ambient gases. Mater Chem Phys 137:372–380
8. Lupan O, Chow L, Chai G, Schulte A, Park S, Heinrich H (2009) A rapid hydrothermal synthesis of rutile SnO_2 nanowires. Mater Sci Eng B 157:101–104
9. Paulo G, Mendes Mario L, Moreira Tebcherani S M, Orlandi MO, Andrés J, Li MS, Mora ND, Varela JA, Longo E (2012) SnO_2 nanocrystals synthesized by microwave-assisted hydrothermal method: towards a relationship between structural and optical properties. J Nanopart Res 14:1–13
10. Jitianu A, Altindag Y, Zaharescu M, Wark M (2003) New SnO_2 nano-clusters obtained by sol–gel route, structural characterization and their gas sensing applications. J Sol–Gel Sci 26:483–488
11. Talebian N, Zavvare HSH (2014) Enhanced bactericidal action of SnO_2 nanostructures having different morphologies under visible light: influence of surfactant. J Photochem Photobiol B 130:132–139
12. Kaneti YV, Yue J, Moriceau J, Chen C, Liu M, Yuan Y, Jiang X, Yu A (2015) Experimental and theoretical studies on noble metal decorated tin oxide flower-like nanorods with high ethanol sensing performance. Sensor Actuator B Chem 219:83–93
13. Pal J, Chauhan P (2009) Structural and optical characterization of tin dioxide nanoparticles prepared by a surfactant mediated method. Mater Charact 60:1512–1516
14. Lupan O, Chow L, Chai G, Heinrich H, Park S, Schulte A (2009) Synthesis of one-dimensional SnO_2 nanorods via a hydrothermal technique. Phys E 41:533–536
15. Azham A, Ahmed AS, Habib SS, Naqvi AH (2012) Effect of Mn doping on the structural and optical properties of SnO_2 nanoparticles. J Alloys Compd 523:83–87
16. Nehru LC, Swaminathan V, Sanjeeviraja C (2012) Photoluminescence studies on nanocrystalline tin oxide powder for optoelectronic devices. Am J Mater Sci 2:6–10
17. Anandan K, Rajendiran V (2010) Size controlled synthesis of SnO_2 nanoparticles: facile solvothermal process. J Non-oxide Glasses 2:83–89
18. Gnanam S, Rajendran V (2010) Synthesis of tin oxide nanoparticles by sol–gel process: effect of solvents on the optical properties. J Sol–Gel Sci Technol 53:555–559
19. Ahmed AS, Muhamed SM, Singla ML, Tabassum S, Naqvi AH, Azam A (2011) Band gap narrowing and fluorescence properties of nickel doped SnO_2 nanoparticles. J Lumin 131:1–6
20. Vijayarangamuthu K, Rath S (2014) Modification of the structural and optical properties of tin oxide nanoparticles by Co doping and thermal annealing. Appl Phys A 114:1181–1188
21. Fang HT, Sun X, Qian LH, Wang DW, Li F, Chu Y, Wang FP, Cheng HM (2008) Synthesis of tin (II or IV) oxide coated multiwall carbon nanotubes with controlled morphology. J Phys Chem C 112:5790–5794
22. Donaldson JD, Moser W, Simpson WB (1963) Basic tin (II) chloride. J Chem Soc 321:1727–1731
23. Li L, Chen S, Xu L, Bai Y, Nie Z, Liu H, Qi L (2014) Template-free synthesis of uniform mesoporous SnO2 nanospheres for efficient phosphopeptide enrichment. Mater Chem B 2:1121–1124
24. Mohagheghia MB, Shahtahmasebi N, Alinejad MR, Youssefi A, Saremi MS (2008) The effect of the post-annealing temperature on the nano-structure and energy band gap of SnO_2 semiconducting oxide nano-particles synthesized by polymerizing–complexing sol–gel method. Phys B 403:2431–2437

25. Cullity BD, Stock SR (2001) Elements of X-ray diffraction, 3rd edn. Prentice Hall, New York
26. Gnanam S, Rajendran V (2010) Anionic, cationic and nonionic surfactants-assisted hydrothermal synthesis of tin oxide nanoparticles and their photoluminescence property. Dig J Nanomater Biostruct 5:623–628
27. Gajendiran J, Rajendran V (2012) Different surfactants assisted on the synthesis of SnO_2 nanoparticles and their characterization. Int J Mater Biomater Appl 2:37–40
28. Gu F, Wang SF, Lu MK, Zhou GJ, Xu D, Yuan DR (2004) Photoluminescence properties of SnO_2 nanoparticles synthesized by sol–gel method. J Phys Chem B 108:8119–8123
29. Periathai RS, Pandiyarajan J, Jeyakumaran N, Prithivikumaran N (2014) Role of temperature on the properties of SnO_2 nanoparticles synthesised by sol–gel process. IJCRGG 3:2132–2134
30. Tauc J, RGrigovici R (1974) Liquid semiconductors. Plenum Press, London
31. Bertoluzza A, Fagnano C, Morelli MA (1982) Raman and infrared spectra on silica gel evolving towards glass. J Non-cryst Solids 48:117–128
32. Tazikeh S, Akbari A, Talebi A, Talebi E (2014) Synthesis and characterization of tin oxide nanoparticles via the Co-precipitation method. Mater Sci Pol 32:98–101
33. Gundrizer TA, Davydov AA (1975) IR spectra of oxygen adsorbed on SnO_2. React Kinet Catal Lett 3:63–70
34. Srinivas K, Rao SM, Reddy PV (2011) Structural, electronic and magnetic properties of $Sn_{0.95}Ni_{0.05}O_2$ nanorods. Nanoscale 3:642–653
35. Rao CNR (1963) Chemical applications of infrared spectroscopy. Wiley, New York
36. Zhang G, Liu M (1999) Preparation of nanostructured tin oxide using a sol–gel process based on tin tetrachloride and ethylene glycol. J Mater Sci 34:3213–3219
37. Luo SH, Wan Q, Liu WL, Zhang M, Song ZT, Lin CL, Chu PK (2005) Photoluminescence properties of SnO_2 nano whiskers grown by thermal evaporation. Prog Solid State Chem 33:287–292